Evaluation and modeling of lanthanum diffusion in TiN/La2O3/HfSiON/SiO2/Si high-k stacks

Zahi Essa, Clement Gaumer, Ardechir Pakfar, Mickael Gros-Jean, Marc Juhel, Federico Panciera, Pierre Boulenc, Clement Tavernier, Fuccio Cristiano

Applied Physics Letters

Evaluation and modeling of lanthanum diffusion in TiN/La_2O_3/HfSiON/SiO_2/Si high-k stacks

Cite as: Appl. Phys. Lett. **101**, 182901 (2012); https://doi.org/10.1063/1.4764558
Submitted: 14 August 2012 • Accepted: 15 October 2012 • Published Online: 29 October 2012

Z. Essa, C. Gaumer, A. Pakfar, et al.

Evaluation and modeling of lanthanum diffusion in $TiN/La_2O_3/HfSiON/SiO_2/Si$ high-k stacks

Z. Essa,[1,2,a)] C. Gaumer,[1] A. Pakfar,[1,b)] M. Gros-Jean,[1] M. Juhel,[1] F. Panciera,[1] P. Boulenc,[1] C. Tavernier,[1] and F. Cristiano[2]
[1]*STMicroelectronics, 850 rue Jean Monnet, F-38926 Crolles, France*
[2]*LAAS CNRS, 7 avenue du Colonel Roche, 31077 Toulouse, France*

(Received 14 August 2012; accepted 15 October 2012; published online 29 October 2012)

In this study, $TiN/La_2O_3/HfSiON/SiO_2/Si$ gate stacks with thick high-k (HK) and thick pedestal oxide were used. Samples were annealed at different temperatures and times in order to characterize in detail the interaction mechanisms between La and the gate stack layers. Time-of-flight secondary ion mass spectrometry (ToF-SIMS) measurements performed on these samples show a time diffusion saturation of La in the high-k insulator, indicating an La front immobilization due to LaSiO formation at the high-k/interfacial layer. Based on the SIMS data, a technology computer aided design (TCAD) diffusion model including La time diffusion saturation effect was developed. © *2012 American Institute of Physics*. [http://dx.doi.org/10.1063/1.4764558]

In order to reduce power consumption in the sub-32 nm complementary MOS (CMOS) technologies, high-k (HK) dielectric materials in association with metal gates (MG) materials are used.[1] HK materials with high permittivity are used as gate dielectrics because they exhibit a low equivalent oxide thickness (EOT) while keeping a higher physical thickness when compared to silicon oxides (SiO_2), therefore reducing gate leakage currents. Over the last years, hafnium oxides (HfO_2, $HfSiO_2$, and HfSiON) deposited on a thin pedestal SiO_2 (or SiON) interfacial layer (IL) have become a serious industrial alternative to classical SiO_2 dielectrics.[2,3] On the other hand, the use of MG materials eliminates the polycrystalline silicon (poly-Si) depletion effect that increases the EOT. However, while tuning the poly-Si doping allows to modify the effective work function (EWF) and to provide adequate threshold voltages (V_t) for both n-MOS and p-MOS transistors, the use of MGs does not allow to easily modify the EWF. A solution to this problem is given by the introduction of a thin capping layer of a rare-earth oxide material between the MG and the HK dielectric.[4,5]

In n-MOS transistors, lanthanum oxide (La_2O_3) is used to provide a negative shift in the V_t. The physical effect behind the negative V_t shift is that in a gate-first approach, the HK and MG are deposited before the fast high temperature spike anneal used for source and drain dopant activation. During the spike anneal, lanthanum atoms diffuse from the La_2O_3 capping layer through the HK and form lanthanum silicates (LaSiO bonds) at the HK/IL interface.[6–8] The LaSiO bonds are believed to form electrical dipoles at the HK/IL interface, which are responsible of the V_t shift.[5,9,10] Thus, the V_t shift is expected to be related to the number of LaSiO dipoles resulting from the La diffusion threw the HK and the LaSiO formation reaction at the HK/IL interface. However, technology relevant n-MOS MG-HK stacks such as $TiN/La_2O_3/HfSiON/SiO_2/Si$ use ultra-thin HK and IL (<3 nm). This makes difficult the study of the La diffusion and reaction mechanisms described above, even though some interesting results were found using electron energy loss spectroscopy, x-ray photoelectron spectroscopy and high resolution transmission electron microscopy.[8] In this work, dedicated gate stack test structures ($TiN/La_2O_3/HK/IL/Si$) with thick HK and IL were intentionally used in order to more reliably investigate the different physical mechanisms occurring during La diffusion in the HK stack. A La diffusion model was finally developed based on the experimental investigations.

The $TiN/La_2O_3/HK/IL/Si$ stacks were prepared using a gate-first approach on 300 mm Si (100) wafers. In order to study the diffusion and reaction mechanisms in the HK and IL, we used two series of samples: (i) "thick" HK (15 nm) on "thick" IL (10 nm) and (ii) "thin" HK (2.5 nm) on "thicker" IL (20 nm). Series (i) and (ii) samples allow us to study the diffusion mechanisms, respectively, in the HfSiON HK and the SiO_2 IL.

Initial silicon substrate was cleaned using a hydrofluoric acid solution. A rapid thermal oxidation of the silicon substrate at 1100 °C and 1150 °C were used to form a 10 nm and 20 nm thick silicon oxide SiO_2 layer, respectively, for series (i) and (ii) samples. The 2.5 nm HfSiON film of series (ii) was deposited by metal organic chemical vapor deposition (MOCVD) of HfSiO followed by a decoupled plasma nitridation (DPN) for 90 s in order to inject nitrogen N in the HK layer. For series (i) samples with a 15 nm HfSiON layer, the HfSiO MOCVD and DPN steps were repeated 6 times. In order to homogenize the N density in the HfSiON, a post nitridation anneal was used for both thin and thick HK samples. Following the IL and HK deposit steps, a 1 nm La_2O_3 capping layer was formed by physical vapor deposition (PVD). A 6.5 nm TiN MG was then deposited by PVD. Finally, thermal anneals at different times and temperatures including 1000 °C/50 s and (1040 and 1080 °C)/(10, 30, and 50 s) were made in order to study the La diffusion and reaction mechanisms in the stack.

The samples were analyzed by time-of-flight secondary ion mass spectrometry (ToF-SIMS) using a 500 eV 45° tilted O_2 beam in order to detect the La^+, HfO^+, Si^+, and Ti^+ clusters signals versus depth. The La intensity quantification was

a)Electronic mail: zahi.essa@st.com.
b)Present address: GlobalFoundries, Dresden, Germany.

done using a reference sample (not shown here) analyzed by atom probe microscopy. The etch rates during ToF-SIMS measurements are different for the stack's different materials. Thus, for series (i) samples where a thick HK was used, depth calibration was made for the HfSiON based on its process thickness (15 nm). The other materials thicknesses are less accurate, however this does not represent a major issue in our study of La diffusion in HfSiON.

For series (ii) samples with a thin HK (2.5 nm) on a thicker IL (20 nm), SIMS results are more difficult to interpret. LaSiO formation after anneal may be important in this case due to the proximity of the HK/IL interface from the La_2O_3 layer forming a thin layer of LaSiO leading to a more difficult La concentration and depth calibration. In addition, following the HfSiON thin layer etch by the SIMS beam, a part of the Hf atoms form a metallic aggregate at the $HfSiON/SiO_2$ interface, which leads to a lower etch rate of the SiO_2 material, therefore, complicating the SIMS calibration and interpretation for series (ii) samples.

Thick HK/thick IL corresponding to series (i) samples were first analyzed. Figure 1 shows the La^+, Ti^+, and HfO^+ clusters intensities versus depth for the as-deposited sample, where we can clearly distinguish the positions and thicknesses of the different layers of the stack. We can notice that the different species profiles are slightly spread in neighboring layers, which is due to SIMS resolution artifacts at the different interfaces, the real intensity profiles being more rectangular. The annealed samples SIMS profiles are shown in Fig. 2. Isochronal anneals (50 s) between 1000 °C and 1080 °C indicate that La diffusion increases in the temperature interval (see Fig. 2(a)) suggesting that the La diffusion mechanism is thermally activated. Previous literature results[7,11] showed that La diffusion in the HK is rather source limited depending on the concentration of La in the La_2O_3 capping layer. This effect was observed in our samples where we noticed (not shown here) that La concentration in La_2O_3 slightly decreases with annealing temperature. However, in addition to the La_2O_3 source effect and according to our experiments, the thermally activated La transport in the HK cannot be ignored. Isothermal anneals at 1040 °C and 1080 °C are shown in Fig. 2(b). It is found that at both temperatures, La diffusion exhibits a transient behavior and

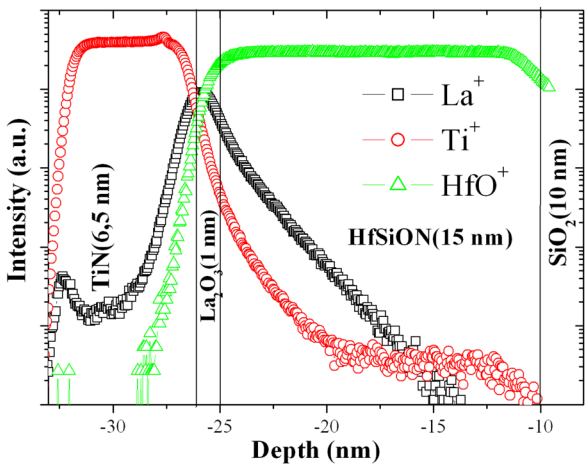

FIG. 1. SIMS profiles including La^+, Ti+, and HfO^+ intensities versus depth of as deposited sample with HfSiON(15 nm)/SiO_2(10 nm).

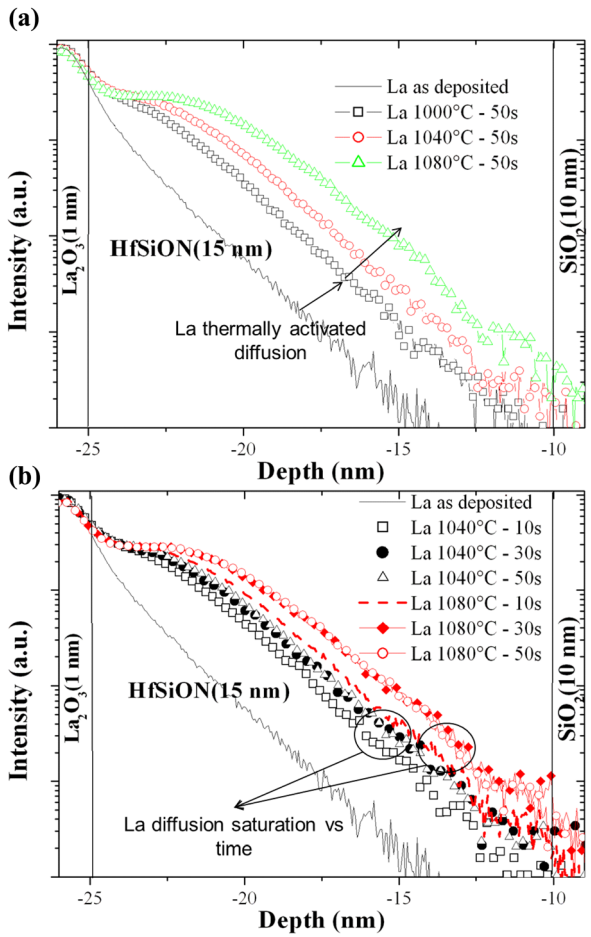

FIG. 2. La SIMS profiles for thermal anneals at (a) 1000, 1040, and 1080 °C during 50 s where we can see that the La diffusion in HfSiON is thermally activated and (b) 1040 and 1080 °C with three different times for each temperature (10, 30, and 50 s) where La diffusion saturation vs. time is observed.

stops after ~30 s. The La diffusion saturation with time in this case is a chemical reaction kinetic effect. Indeed, as mentioned above, La reacts with SiO bonds at the HK/IL interface forming lanthanum silicates LaSiO in a stable phase, probably stopping the La diffusion and explaining the overlapping of 30 and 50 s curves in Fig. 2(b). Consequently, two mechanisms both in agreement with literature results,[6–8] explain SIMS data of Figs. 2(a) and 2(b): a diffusion mechanism of La atoms that is thermally activated and a kinetic reaction mechanism explaining the diffusion saturation versus time due to LaSiO dipoles formation at the HK/IL interface.

Thin HK/thicker IL series (ii) samples were also analyzed. Figure 3 shows that La diffuses after thermal anneals in the HfSiON material compared to the as deposited sample. However, as previously explained, SIMS resolution limits on these thin HK/thick IL samples could not be resolved. Some uncertainties on the positions and depths of the different materials in the stack persisted, so that further modeling based on these data was not possible. In series (ii) samples, given the thickness of the HfSiON (2.5 nm) and the proximity of the HK/IL interface from the La_2O_3 capping layer, the La diffusion saturation occurs probably faster, forming a thin LaSiO layer between the HK and the IL, even after 10 s of anneal.

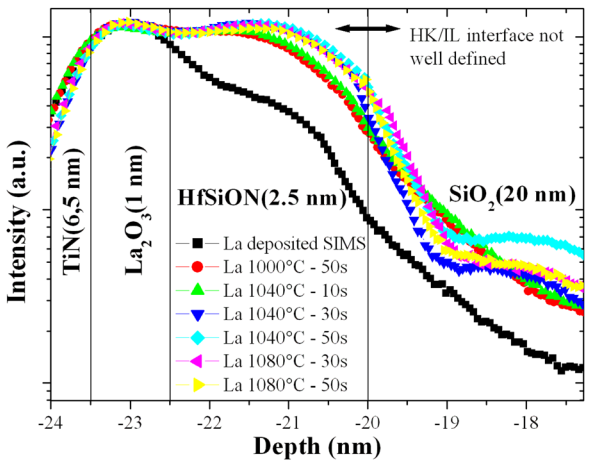

FIG. 3. La SIMS profiles for series (ii) samples with a thin HfSiON (2.5 nm) HK and a thick SiO_2 (20 nm) IL.

In the following, we will concentrate on the evaluation and modeling of La diffusion in the thick HK/thick IL series (i) samples in order to have a better understanding of La diffusion in the TiN/La_2O_3/HfSiON/SiO_2/Si stack. Previously, we assumed that the La diffused profiles can be explained by two mechanisms: a thermally activated diffusion mechanism allowing the La atoms to reach the HK/IL interface and a kinetic reaction mechanism due to LaSiO dipoles formation at the HK/IL interface that blocks the diffusion mechanism explaining diffusion saturation versus time in Fig. 2(b). The simulations will allow us to check the validity of our assumptions. The diffusion model developed here was implemented in Synopsys Sentaurus Process (SProcess) technology computer aided design (TCAD) tool using the scripting language Alagator[12] that is used to define the species and their different related equations in the HfSiON material and at the La_2O_3/HfSiON interface. Our model mainly deals with the diffusion of La in the HfSiON material. The La diffusion equation is, therefore, considered only in this material. Given the SIMS results in the 1 nm La_2O_3 layer where the La concentration is almost unaltered after thermal anneal, a Dirichlet boundary condition[13] is considered at the La_2O_3/HfSiON interface, according to which the La_2O_3 layer is an infinite source emitting La in the HfSiON. A constant La concentration is considered in the La_2O_3 layer that was adjusted to the one measured by SIMS at the La_2O_3/HfSiON for the as-deposited sample. The simplest diffusion equation that can be used for La is Fick's second law[14] described by

$$\frac{\partial La}{\partial t} = D\frac{\partial^2 La}{\partial x^2}, \tag{1}$$

where La is the concentration of lanthanum in cm^{-3} and D is the La diffusivity in $cm^2\ s^{-1}$. Before going further, we should notice that the isotropic diffusivity chosen in Eq. (1) is quite simplistic and assumes that the HK material is amorphous. However, it has already been noticed[15] that for thick HK layers, some partial crystallization may take place after the thermal anneal leading to the formation of crystalline regions within the amorphous HK layer. In this case, La diffusion may be monitored by different complexes, clusters, and grain boundaries formed during the thermal anneal and leading to an anisotropic diffusivity. Therefore, if the partial crystallization is confirmed, the diffusivity D in Eq. (1) should be considered as an effective diffusivity in our one dimensional structures. Figure 4 shows the TCAD simulation results using Eq. (1) for samples annealed at 1040 °C for 10, 30, and 50 s, with D fixed at 6.10^{-15} $cm^2\ s^{-1}$. As expected when using Fick's second law of Eq. (1), the longer the anneal time, the more La diffuses. This does not correspond to the experiments (see Fig. 2(b)) indicating diffusion saturation versus time of anneal. La reaction from the La_2O_3 capping layer with SiO bonds from the HfSiON HK and the SiO_2 IL are quite complex and related to the phase diagram for the La_2O_3.SiO_2 binary system.[16] We simplify the different chemical reactions leading to the LaSiO formation at the HK/IL interface using the following reaction:

$$La + SiO \xrightarrow{k_f} LaSiO, \tag{2}$$

where k_f is the forward LaSiO formation reaction constant. Reaction 2 limits the diffusion of La in the HfSiON and in order to further simplify our model, we consider that the reaction takes place in all the material and not only at the HK/IL interface. Considering that a La infinite source was considered with the Dirichlet boundary condition at the La_2O_3/HfSiON interface, La is not a limiting factor for reaction 2, and SiO bonds follow the 1st order differential equation:

$$\frac{dSiO}{dt} = k_f\, SiO, \tag{3}$$

whose analytical solution is: $SiO(t) = SiO(t=0)e^{-k_f t}$, where SiO(t = 0) is the concentration of SiO bonds at the initial time of anneal. Thus, defining S(t) as the unitless function:

$$S(t) = \frac{SiO(t)}{SiO(t=0)} = e^{-k_f t}, \tag{4}$$

one can reproduce the diffusion saturation versus time taking into account reaction 2 by modifying La Fick's 2nd law diffusion Eq. (1):

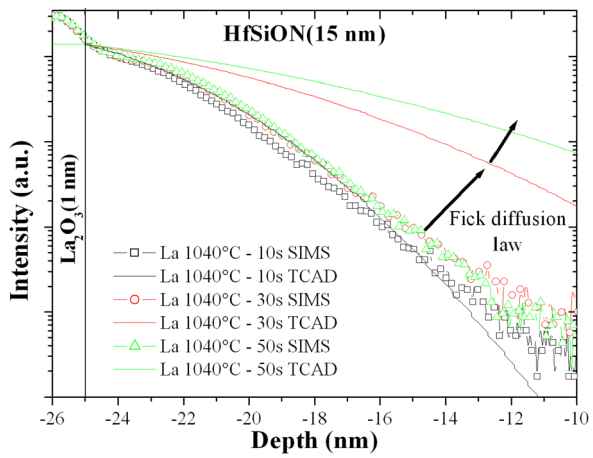

FIG. 4. La SIMS versus TCAD profiles for thermal anneal at 1040 °C during 10, 30, and 50 s, using Eq. (1) where La diffusion saturation versus time in not correctly reproduced.

$$\frac{\partial La}{\partial t} = D.S(t)\frac{\partial^2 La}{\partial x^2}. \quad (5)$$

We should notice that $S(t=0)=1$ and $S(t) \underset{t\to\infty}{\longrightarrow} 0$ and thus the effective diffusivity D.S(t) will tend towards 0 versus time, which will block the diffusion mechanism and will reproduce the diffusion saturation versus time. The La diffusion model represented by Eqs. (3)–(5) has been calibrated on the different SIMS data and the best agreement was obtained with D fixed at $1.25.10^{-10}e^{-\frac{1.04(eV)}{k_BT}}$cm^2 s^{-1} and k_f at 0.15 s^{-1}, where k_B is the Boltzmann constant and T is the temperature in °C. The results of the TCAD simulations are shown in Fig. 5. As we can see on Fig. 5(a), diffusion saturation at 1040 °C is correctly modeled. Diffusion saturation versus time at 1080 °C (not shown) was also correctly modeled. Thus, our hypothesis concerning a kinetic effect due to the formation of LaSiO dipoles has been verified. On the other side, the diffusivity D follows an Arrhenius law versus temperature, and the thermally activated diffusion mechanism is also verified. The thermally activated diffusion mechanism represented in Fig. 5(b) shows a good agreement between TCAD and SIMS results in the tails of the La diffused profiles. However, the agreement between simulations and experiments worsen near the La_2O_3/HfSiON interface. Actually, we can observe that near the La_2O_3/HfSiON interface, where the La concentration is very high, La diffusion is stronger than far from the interface where La concentration is lower. In addition, the La diffusivity for high La concentration increases with temperature. Thanks to the simulations, we were able to reproduce this effect using the following improved La diffusion equation:

$$\frac{\partial La}{\partial t} = D\left(S(t) + \frac{La}{La_0}\right)\frac{\partial^2 La}{\partial x^2}, \quad (6)$$

with S(t) already defined in Eq. (4) and La_0 is a fitting parameter. Equation (6) parameters have been calibrated using the SIMS data: k_f kept the same value 0.15 s^{-1} as in Eq. (5), D has been slightly changed to $1.2.10^{-10}e^{-\frac{1.04(eV)}{k_BT}}$cm^2 s^{-1} and the La_0 fitting parameter has been fixed at $1.91.10^{12} \times e^{\frac{2.92(eV)}{k_BT}}$cm^{-3}. TCAD simulations results are presented in Fig. 6. Fig. 6(a) shows that the diffusion saturation effect is correctly modeled using Eq. (6) for 1040 °C (not shown) and 1080 °C as we have already seen in Fig. 5(a) using Eq. (5). The La thermally activated diffusion mechanism is correctly modeled in the tail of the profiles, but also near the La_2O_3/HfSiON interface thanks to the La/La_0 term enhancing the La diffusion in the high La concentration region and at high

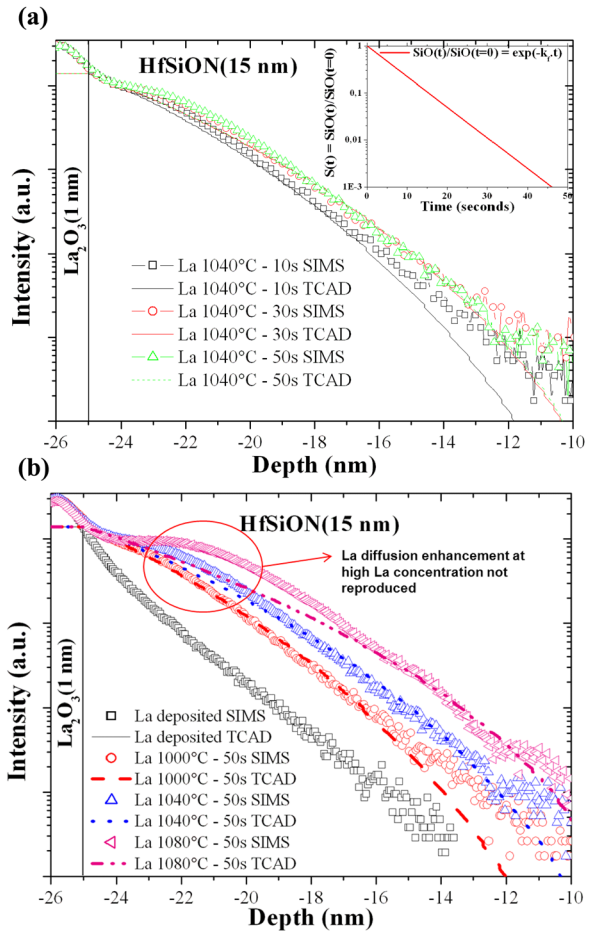

FIG. 5. La SIMS versus TCAD profiles for thermal anneals at (a) 1040 °C during 10, 30, and 50 s, using Eq. (5) where La diffusion saturation versus time is correctly reproduced and (b) at 1000, 1040, and 1080 °C during 50 s, using Eq. (5) where La thermally activated diffusion is correctly reproduced, except near the La_2O_3/HfSiON interface with a high La concentration.

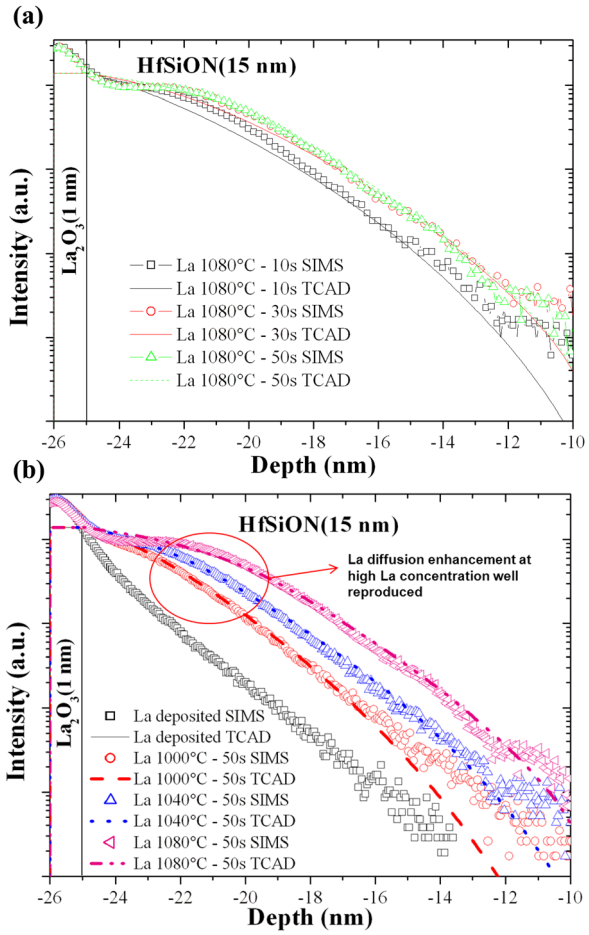

FIG. 6. La SIMS versus TCAD profiles for thermal anneal at (a) 1080 °C during 10, 30, and 50 s, using Eq. (6) where La diffusion saturation versus time is correctly reproduced and (b) at 1000, 1040, and 1080 °C during 50 s, using Eq. (6) where La thermally activated diffusion is correctly reproduced, including near the La_2O_3/HfSiON interface with a high La concentration.

temperatures. Thus, we can see on Fig. 6(b) a very good agreement between experimental and simulated results. This one dimensional La diffusion model in HfSiON of Eq. (6) can be easily extended to two and three dimensions and coupled with a device dipole model in order to predict V_t shifts in n-MOS transistors as a function of the number of LaSiO dipoles formed at the HfSiON/SiO_2 interface following a given thermal budget. Yet, it should be noticed that for a thinner HK layer as the one in series (ii), we may have a predominance of the reaction mechanism and the formation of a lanthanum silicates LaSiO layer between the HK and IL. Thus, the diffusion model developed here for thick HK should be supplemented by a growth reaction model as in Ref. 17 for the formation of LaSiO layer at the HK/IL interface in our case.

In this work, we studied the La diffusion after high temperature dopant activation anneal in TiN/La_2O_3/HfSiON/SiO_2/Si HK stacks of n-MOS transistors that are used to get a negative shift of the V_t threshold voltage following the formation of LaSiO dipoles at the HfSiON(HK)/SiO_2(IL) interface. We used ToF-SIMS measurements on high-k stacks with thick HK and IL, annealed at different temperatures and times, in order to evaluate La diffusion in the different materials of the stacks. The thick HK/thick IL SIMS data allowed us to observe two mechanisms explaining the diffused La profiles: a thermally activated diffusion mechanism leading to the migration of La from the La_2O_3 capping layer to the HfSiON(HK)/SiO_2(IL) interface and a kinetic reaction mechanism due to the LaSiO dipoles formation at the same interface and explaining the La diffusion saturation versus time. A TCAD diffusion model was developed and allowed us to confirm these two mechanisms.

We want to thank STMicroelectronics Crolles high-k dielectrics deposition team and physical characterization team for the preparation and SIMS measurements of the different samples. The research leading to these results has received funding from the European Union Seventh Framework Program (FP7/2007-2013) under Grant Agreement No. 258547 (ATEMOX).

[1]G. D. Wilk, R. M. Wallace, and J. M. Anthony, J. Appl. Phys. **89**, 5243–5275 (2001).
[2]B. H. Lee, L. Kang, W. J. Qi, R. Nieh, Y. Jeon, K. Onishi, and J. Lee, Tech. Dig.—Int. Electrons Devices Meet. **1999**, 133–136.
[3]M. A. Quevedo-Lopez, S. A. Krishnan, P. D. Kirsch, G. Pant, B. E. Gnade, and R. M. Wallace, Appl. Phys. Lett. **87**, 262902 (2005).
[4]V. Narayanan, V. K. Paruchuri, N. Bojarczuk, B. P. Linder, B. Doris, Y. H. Kim, S. Zafar, J. Stathis, S. Brown, J. Arnold, M. Copel, M. Steen, E. Cartier, A. Callegari, P. Jamison, J. P. Locquet, D. Lacey, Y. Wang, P. E. Batson, P. Ronsheim, R. Jammy, M. P. Chudzik, M. Ieong, S. Guha, G. Shahidi, and T. C. Chen, Dig. Tech. Pap.—Symp. VLSI Technol. **2006**, 178–179.
[5]P. D. Kirsch, P. Sivasubramani, J. Huang, C. D. Young, M. A. Quevedo-Lopez, H. C. Wen, H. Alshareef, K. Choi, C. S. Park, K. Freeman, M. M. Hussain, G. Bersuker, H. R. Harris, P. Majhi, R. Choi, P. Lysaght, B. H. Lee, H. H. Tseng, R. Jammy, T. S. Boscke, D. J. Lichtenwalner, J. S. Jur, and A. I. Kingon, Appl. Phys. Lett. **92**, 092901 (2008).
[6]H. N. Alshareef, M. Quevedo-Lopez, H. C. Wen, R. Harris, P. Kirsch, P. Majhi, B. H. Lee, R. Jammy, D. J. Lichtenwalner, J. S. Jur, and A. I. Kingon, Appl. Phys. Lett. **89**, 232103 (2006).
[7]E. Martinez, P. Ronsheim, J. P. Barnes, N. Rochat, M. Py, M. Hatzistergos, O. Renault, M. Silly, F. Sirotti, F. Bertin, and N. Gambacorti, Microelectron. Eng. **88**, 1349–1352 (2011).
[8]R. Boujamaa, S. Baudot, N. Rochat, R. Pantel, E. Martinez, O. Renault, B. Detlefs, J. Zegenhagen, V. Loup, F. Martin, M. Gros-Jean, F. Bertin, and C. Dubourdieu, J. Appl. Phys. **111**, 054110 (2012).
[9]K. Kita and A. Toriumi, Appl. Phys. Lett. **94**, 132902 (2009).
[10]L. Lin and J. Robertson, J. Appl. Phys. **109**, 094502 (2011).
[11]M. Copel, S. Guha, N. Bojarczuk, E. Cartier, V. Narayanan, and V. Paruchuri, Appl. Phys. Lett. **95**, 212903 (2009).
[12]Synopsys Sentaurus Process User Guide, Version E-2010.12, Synopsys Inc., Mountain View, CA (2010).
[13]A. Cheng and D. T. Cheng, Eng. Anal. Boundary Elements **29**, 268–302 (2005).
[14]A. Fick, Ann. Phys. **170**(1), 59–85 (1855).
[15]M. A. Quevedo-Lopez, S. A. Krishnan, P. D. Kirsch, H. J. Li, J. H. Sim, C. Huffman, J. J. Peterson, B. H. Lee, G. Pant, B. E. Gnade, M. J. Kim, R. M. Wallace, D. Guo, H. Bu, and T. P. Ma, Tech. Dig.—Int. Electrons Devices Meet **2005**, 428.
[16]J. P. Maria, D. Wicaksana, A. I. Kingon, B. Busch, H. Schulte, E. Garfunkel, and T. Gustafsson J. Appl. Phys. **90**, 3476–3482 (2001).
[17]D. Gopireddy and C. G. Takoudis, Phys. Rev. B **77**, 205304 (2008).